Research article

Microstructure and mechanical properties of newly developed SiC-C/C composites under atmospheric conditions

Kiyotaka Obunai[1],*, Daisuke Mikami[2], Tadao Fukuta[3] and Koichi Ozaki[3]

[1] Faculty of Science and Engineering, Doshiaha University, JAPAN
[2] Graduate school of Okayama Prefectural University, JAPAN
[3] Faculty of Computer Science and System Engineering Okayama Prefectural University, JAPAN

* Correspondence: Email: kiobunai@mail.doshisha.ac.jp; Tel: +81774656972.

Abstract: The purpose of this study is to investigate the relationship between its microstructure and bending strength of SiC-C/C (carbon-carbon) composites. By using the phenolic resin and carbon fiber bundle, the carbon fiber reinforced plastics (CFRP) precursor was prepared by employing filament winding technique. To modify the phenolic resin, the micro-sized glass fiber was added. The CFRP precursor was charred at high temperature at Argon atmosphere to obtain SiC-C/C composites. The matrix of composites was densified by resin impregnation done by cold isostatic pressing (CIP) method. The detail observation of matrix after charred revealed that when precursor resin was modified with glass fiber, the direction of thermal crack at matrix showed complex manner, while thermal crack at un-modified matrix only appeared along fiber direction. Because of the presence of complex thermal crack, the matrix of SiC-C/C composite showed high porosity at un-densified condition and effectively densified by CIP to promoting resin flow toward thermal crack. The bending and compression test results showed that bending strength and inter-laminar shear strength of SiC-C/C composites was increased by densification. Moreover, the fractured surface observations suggested that the presence of synthesized SiC nano-whisker at inter-laminar enhances the apparent shear strength due to mechanical bridging between laminar.

Keywords: SiC-C/C composites; densification; bending strength; inter-layer shear strength

1. Introduction

Carbon fiber reinforced carbon composite materials (C/C composites) are a class of advanced

composite materials well known for their high durability in high-temperature environments [1]. Nowadays, the C/C composites are mainly used for vital parts of space vehicles, such as rocket nozzles and heat shields [2,3]. When considering the application of C/C materials under atmospheric conditions, the oxidation of the C/C composites must be avoided to prevent the degradation of their mechanical and physical characteristics [4,5]. One way to avoid the oxidation of these composites is to modify the carbon matrix with oxidation resistant materials such as SiC. In order to modify the carbon matrix, researchers have examined many techniques such as modifier impregnation and modification by the chemical vapor deposition (CVD) process [6–8]. By conducting the modification of carbon matrix, previous studies reported that the change in frictional coefficient cause by the oxidation of composites was effectively reduced [9–11]. However, these conventional processes not only require long processing times but may also introduce flaws into the composites during the modification process [12]. To solve these problems, one of the authors has proposed a novel method, where modification and graphitization of the carbon matrix were carried out simultaneously [13,14]. By employing this method, much of the processing time required for SiC modification could be eliminated. Moreover, previous studies of the authors have revealed that SiC nano-whiskers could be synthesized in the carbon matrix by the addition of solid modifiers such as micro-sized glass fibers into the carbon precursor, while conventional modification techniques such as CVD yield the SiC phase only at the surface of the composites. The authors also revealed that the synthesized SiC nano-whiskers improve the mechanical properties and tribological characteristics of the composites [15]. In this research, the effect of this proposed modification method on the microstructures of C/C composites is studied, particularly in terms of the pores formed during the charring process. The densification availability of the composites prepared by the proposed method and its effect on mechanical properties were also investigated. In this paper, among of the mechanical properties of composites, the bending strength and inter-laminar shear strength were mainly investigated; because of the ceramic matrix composites are rather susceptible to inter-laminar failure in the matrix [16,17].

The purpose of this study is to investigate the relationship between the microstructure and bending strength of developed SiC-C/C composites. The micro-sized glass fibers were dispersed in phenolic resin before impregnation into a pitch-based carbon fiber bundle. The impregnated bundle was wound to a bobbin by employing a filament winding technique to fabricate a carbon fiber reinforced plastics (CFRP) precursor. The CFRP precursor was charred at a high temperature under an Argon atmosphere to obtain SiC-C/C composites. The matrix of the composites was densified by the repeated charring of the resin impregnated by the cold isotropic pressing (CIP) method. The pore diameter and volume in the composites were investigated by mercury porosimetry. The mechanical properties of the composites were characterized using a four-point bending test. The inter-laminar shear strength of the composites was also investigated by compression testing with a double-notched specimen.

2. Materials and methods

2.1. Materials

A resol-type phenolic resin (PHENOLITE 5010: DIC) was used as the carbon precursor resin, which is the base material that forms the matrix of the SiC-C/C composite, and a 3 K pitch carbon

fiber bundle (XN-20-30S: Japan graphite fiber) was used as the reinforcement material. In addition, a milled glass fiber (EFH 100-31 Central Glass Fiber) in which the fiber diameter and length were 11 and 100 μm, respectively, was used as an additive. Table 1 shows the mechanical characteristics of the raw materials. Table 2 also shows the chemical composition of the glass fibers.

Table 1. Properties of materials.

	Phenolic resin	Carbon fiber	Glass fiber
Density [g/cm^3]	1.05	1.98	2.55
Elastic modulus [GPa]	-	196	72.6
Tensile strength [MPa]	-	3000	3430

Table 2. Chemical composition of glass fiber (in mass%).

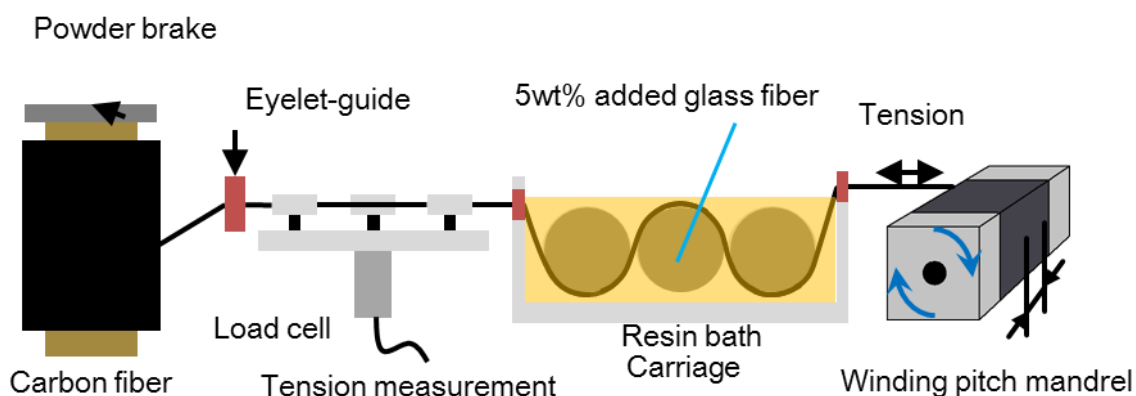| SiO$_2$	Al$_2$O$_3$	CaO	MgO	B$_2$O$_3$	Na$_2$O + K$_2$O
53	15	21	2	8	0.3

Figure 1. Schematic illustration of a filament winding machine.

2.2. Fabrication procedures of SiC-C/C composites

The unidirectional CFRP preform plate was fabricated by employing a filament winding technique. Figure 1 shows the filament winding machine used in this study. The carbon fiber bundle was dipped into the phenolic resin, in which 5.0 wt.% of the glass fiber was uniformly dispersed. The dipped fiber bundle was wound onto a cubic bobbin with a hoop winding configuration under controlled tension and winding pitch. In this study, the tensions applied to the bundle and the winding pitch were 3.5 N and 3.0 mm, respectively. The wound CFRP preform was then dried in an oven at 353 K for 24 h to eliminate any ethanol in the resin. After drying, the box-shaped CFRP preform was cut into its apex to obtain CFRP plates, and these plates were heat pressed at 423 K under 15 MPa for 1 h to cure the phenolic resin matrix. At this time, the fiber volume fraction V_f of the fabricated CFRP preform was about 60%. The fabricated CFRP preform plate was cut parallel to the fiber direction to fabricate $80 \times 15 \times 3$ mm^3 and $80 \times 13 \times 4$ mm^3 coupon-type specimens for bending and compression testing, respectively. The fiber directions of these specimens were aligned with the longitudinal direction of the specimen. To compare the proposed SiC-C/C composites and

the conventional C/C composites, a C/C composite in which the carbon precursor matrix was not modified with glass fibers was fabricated using the same procedure.

To fabricate the SiC-C/C composites, the CFRP preform was subjected to the following two processes to ensure that its carbon precursor matrix was well charred. In the first phase, the preform was heated up to 1273 K at a rate of 1.0 K/min and then kept at that temperature for 1 h in a ring furnace. During the first phase, the phenolic matrix of the CFRP was only carbonized. In the second phase, the preform was heated up to 1773 K at a rate of 1.5 K/min and then kept at that temperature for 1 h. During the second phase, the graphitization of the carbon matrix and the synthesis of SiC proceeded simultaneously. After heating, the preform was cooled gradually. These processes were conducted under argon atmosphere to avoid oxidation. In this phase, no significant differences at cross section of SiC-C/C and C/C were observed in its cross section [13].

2.3. Densification process

The fabricated composites were impregnated with resin in order to fill the pores within the matrix and obtain densified composites. In this study, the CIP technique was employed to impregnate the precursor resin into the porous composites. At first, the un-densified composites and precursor resin were placed in a bag made of PP. Then, the air in the bag was removed by a vacuum pump and the bag was heat sealed tightly. The sealed bag was placed in a pressure vessel, which was then filled with water and sealed. Thereafter, the pressure in the vessel was elevated to 10 MPa and held there for 1 h. After CIP, the bag was removed from the vessel and heated in an oven to cure the precursor resin. After curing, the impregnated composites were heated up to 1273 K at a rate of 1.0 K/min and kept at that temperature for 1 h. The above processes were conducted repeatedly to densify the composites. After densification, the composites were heated up to 1773 K. Hereafter, the test pieces are referred to by the number of densification processes used (e.g., sample CIPn was subjected to n densification processes).

2.4. Measurement of pore distribution

The pore diameters and volumes in the composites were measured using a mercury porosimeter (Micrometrics Instrument, AutoPore V9600). In this study, the applied mercury pressure during measurement was varied from 12.2×10^{-2} to 413 MPa, allowing for the measurement of pore diameters from 3×10^{-3} to 10 μm. The relationship between pore diameter and applied pressure is given by the following Eq 1 [18]:

$$D = \frac{-4\gamma cos\theta}{P}$$
(1)

Here, D, γ, θ, and P denote the diameter of the pore, surface tension of mercury, contact angle between the specimen and mercury, and applied pressure, respectively. In this measurement, γ and θ were considered to be constants, with values of 476 mN/m and 130°, respectively. The applied pressure and the volume impregnated during the test were measured to evaluate the pore diameter and volume in the composites.

2.5. Four-point bending test

The mechanical properties of the composites were characterized using four-point bending loads with a universal testing machine (EZ-L: SHIMADZU Co., Ltd.). The coupon-type specimens of known length, width, and thickness were subjected to a four-point bending test, with the lower span, upper span, and cross head speed set to 51 mm, 17 mm, and 1.0 mm/min, respectively. Bending stress and strain were simply calculated using the Eqs 2 and 3:

$$\sigma_B = \frac{FL}{wt^2} \tag{2}$$

$$\varepsilon_B = \frac{4.7\delta t}{L^2} \tag{3}$$

Here, F, δ, L, w, and t denote the applied bending load, deflection, span, width of specimen, and thickness of the specimen, respectively. At least five specimens were subjected to the test to investigate the bending properties.

2.6. Compression test

The inter-laminar shear strength of the composites was characterized by compression load testing using a universal testing machine (EZ-L: SHIMADZU Co., Ltd.). Figure 2 shows the testing apparatus and specimen for the compression tests.
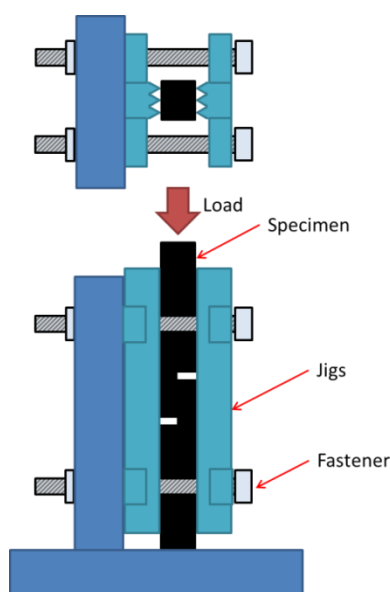

Figure 2. Test apparatus and specimen for the compression test.

To avoid buckling of the specimen, the displacement of the specimen along the thickness direction was constrained by inserting it between jigs with V-shaped grooves on their contact surfaces. The jigs were bolted with 0.02 N·m of tightening torque. To promote shear stress during compression, parallel square notches in alternating directions were machined into the specimen. The inter-laminar shear strength of the composites was calculated using the following Eq 4:

$$\tau = \frac{F_c}{wl} \tag{4}$$

Here, F_c, w, and l denote the maximum compressive force, width of the specimen, and the distance between two notches, respectively. In this study, the distance between two notches was controlled at a constant value of 6.4 mm. The configurations of the test apparatus and specimens were decided by referring to the industrial standard (JIS-K7092). At least five specimens were subjected to the test to investigate the bending properties of the composites.

3. Results and discussions

3.1. Pore structure of composites

In order to evaluate the porosity of the composites, the weight changes during the densification process were first investigated. The macroscopic pore characteristics changed according to the number densification processes used. Figure 3 shows the calculated porosity of the composites as a function of the number of densification processes. The porosity, α, of the composites was calculated using the equations:

$$D_e = \frac{M_s - M_{cf} - M_{SiC}}{\left(1 - V_f - V_{CO_2}\right)\rho_c} \tag{5}$$

$$\alpha = \left(1 - V_f\right)\left(1 - D_e\right) \tag{6}$$

Here, D_e, M_s, M_{cf}, M_{SiC}, V_{CO_2}, and ρ_c denote the degree of densification, weight of the specimen, weight of carbon fiber, weight of synthesized SiC, volume fraction of CO_2, and density of carbon, respectively. In the denominator of Eq 5, the ideal weight of the carbon matrix is calculated. When the matrix was not modified, the volume fraction of the matrix could be calculated by subtracting V_f from one. However, when the matrix was modified to produce SiC, the following synthesis reactions occurred around 1700 K [13]:

$$SiO_2(s) + 3C(s) = SiO(g) + CO(g) \tag{7}$$

$$SiO(g) + 3CO(g) = SiC(s) + 2CO_2(g) \tag{8}$$

As a result of SiC synthesis, gas-phase CO_2 was produced within the matrix. Therefore, the volume fraction of CO_2 must be subtracted to calculate the ideal weight of the carbon matrix. The calculated results show that the porosities of the composites progressively decreased as the number of densification processes was increased. This tendency of the porosity to decrease was observed irrespective of whether the composite matrix was modified or not. Therefore, the developed SiC-C/C composites could be densified in the same fashion as the C/C composites by a conventional CIP process. When comparing the decrease in porosity of each composite prior to densification (CIP0), the porosity of the SiC-C/C composites was higher than that of the C/C composites. However, as the number of densification processes was increased, the difference in porosities between the SiC-C/C and C/C composites decreased.

Figure 4 shows the pore diameter distribution and its specific volume plotted against the weight of the developed SiC-C/C composites and C/C composites. For un-densified composites, a

significant peak at a pore diameter around 2.0 μm was observed for both the composites. However, the pore volume of the un-densified SiC-C/C composite was higher than that of the un-densified C/C composite. The measured results also show that the pore distribution and volume of the well-densified composites were almost the same, irrespective of whether the precursor resin was modified or unmodified.
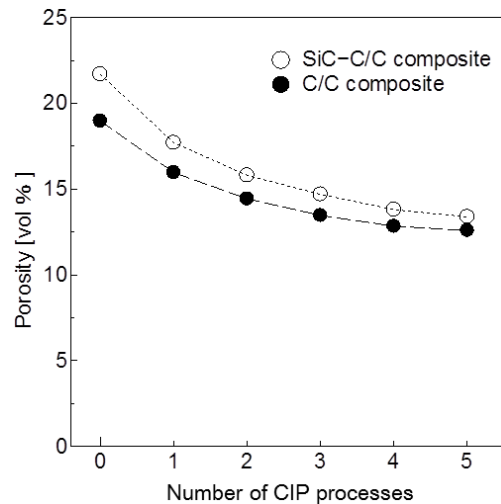

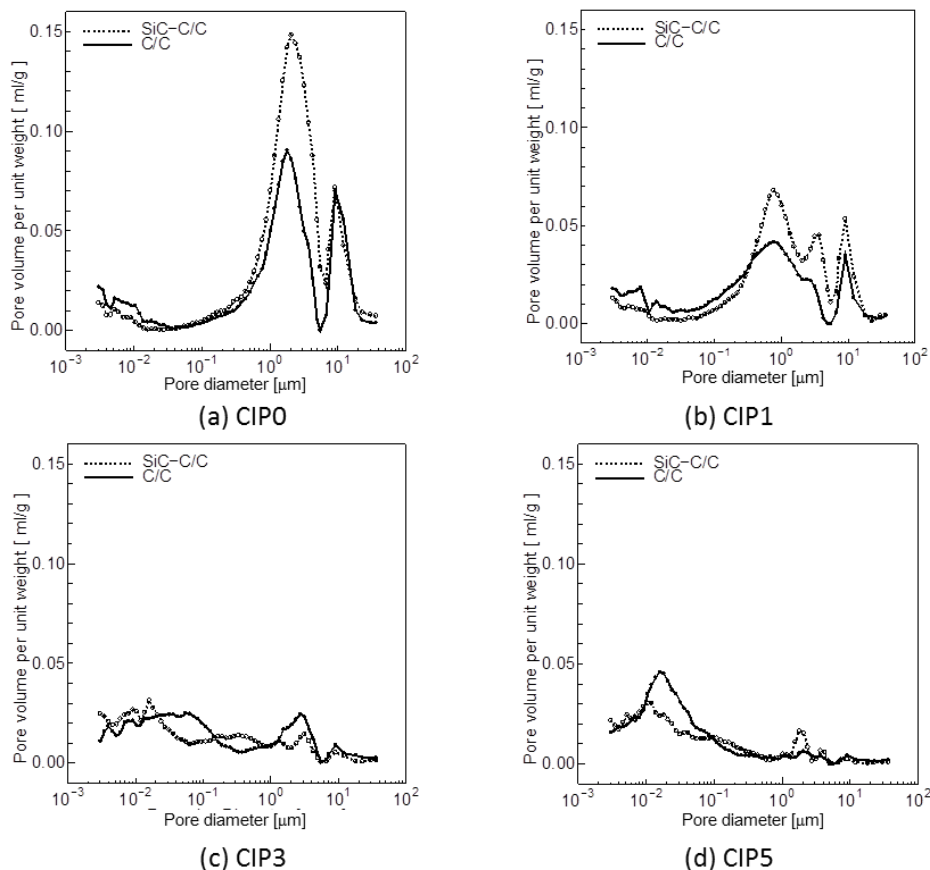**Figure 3.** Porosity as a function of the number of CIP processes.

(a) CIP0

(b) CIP1

(c) CIP3

(d) CIP5

Figure 4. Pore volume per unit weight as a function of pore diameter.

Figure 5 also shows the pore volume change plotted against the number of densification processes. Almost the same tendency was confirmed for the changes in porosity and pore volume. These results suggest that the SiC-C/C composites fabricated by the proposed method could be more effectively densified by a conventional process compared to the C/C composites.
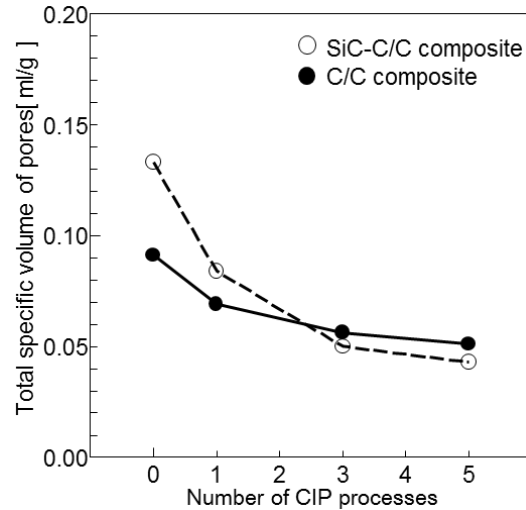

Figure 5. Total specific volume of pores as a function of the number of CIP processes.

3.2. Bending characteristics of composites

Figure 6 shows the typical bending stress–bending strain (σ_B–ε_B) diagrams for both the composites. Figure 7 also shows the bending strength and flexural modulus of both the composites with respect to the number of densification processes.
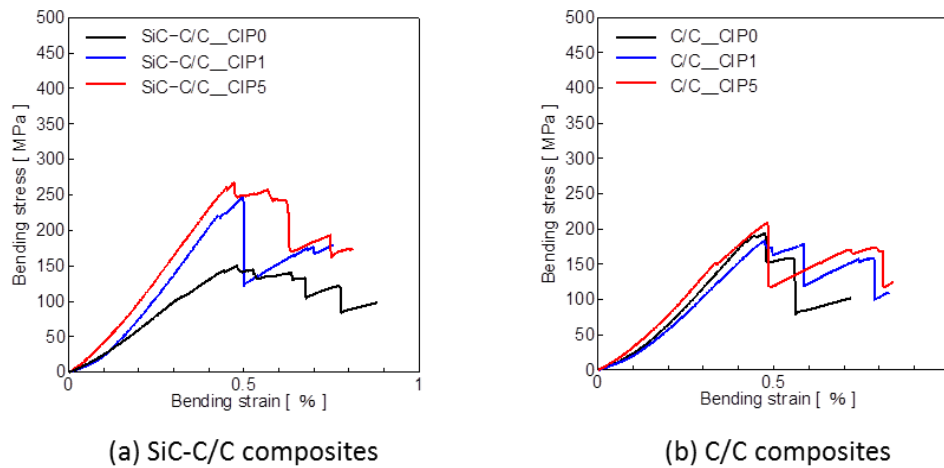

(a) SiC-C/C composites

(b) C/C composites

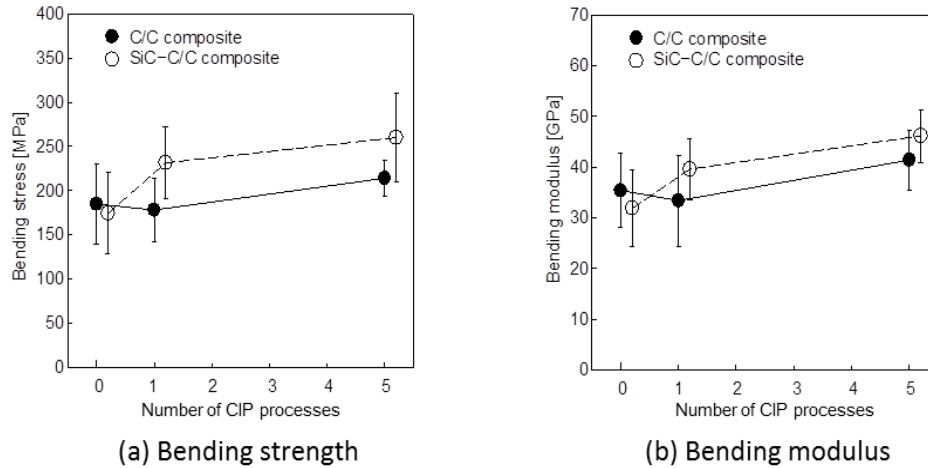**Figure 6.** Typical bending stress–bending strain diagrams.

Figure 7. Change in bending strength and bending modulus with respect to the number of CIP processes.

The σ_B–ε_B diagrams show that the bending stress increased almost linearly until it reached the bending strength, before rapidly decreasing. An observation of the specimens during the bending test also revealed that interlayer shear failure occurred, regardless of whether the matrix was modified or not. The change in bending strength and flexural modulus with respect to the number of densification processes revealed that adding glass fibers to the precursor resulted in greater improvements in bending strength and bending modulus due to densification compared with the C/C composites. These results suggest that applying the densification process to the SiC-C/C composites prepared via the proposed method has effectively improved their bending characteristics.

3.3. Inter-laminar shear strength of composites

Figure 8 shows the typical shear stress–stroke diagrams for both the composites. Figure 9 also shows the inter-laminar shear strength of the composites with respect to the number of densification processes.
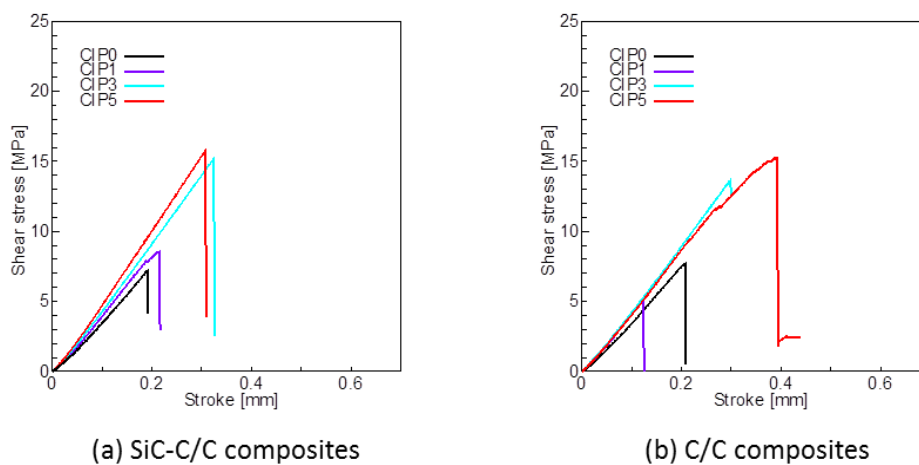

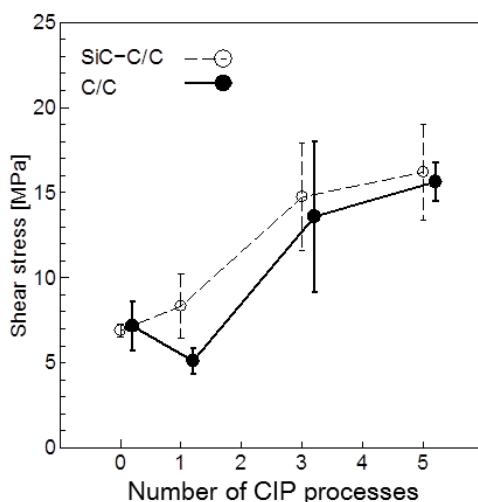**Figure 8.** Typical shear stress–stroke diagrams.

Figure 9. Interlaminar shear strengths of composites with respect to the number of densification processes.

The inter-laminar shear strength of the developed SiC-C/C composites increased with increasing number of densification processes. However, the shear strength of the conventional C/C composite that was densified once decreased. After this initial decrease, the shear strength of the C/C composites was increased with subsequent densification processes. This trend is almost the same as that observed for the bending characteristics of the composites. Therefore, the improvement in the bending characteristics of the composites could be explained by the improvement in their inter-laminar shear strengths. Comparing SiC-C/C and C/C composites, the inter-laminar shear strength of the SiC-C/C composites was a little higher than that of the C/C composites. Figures 10 and 11 show the fractured surfaces observed from both the composites.
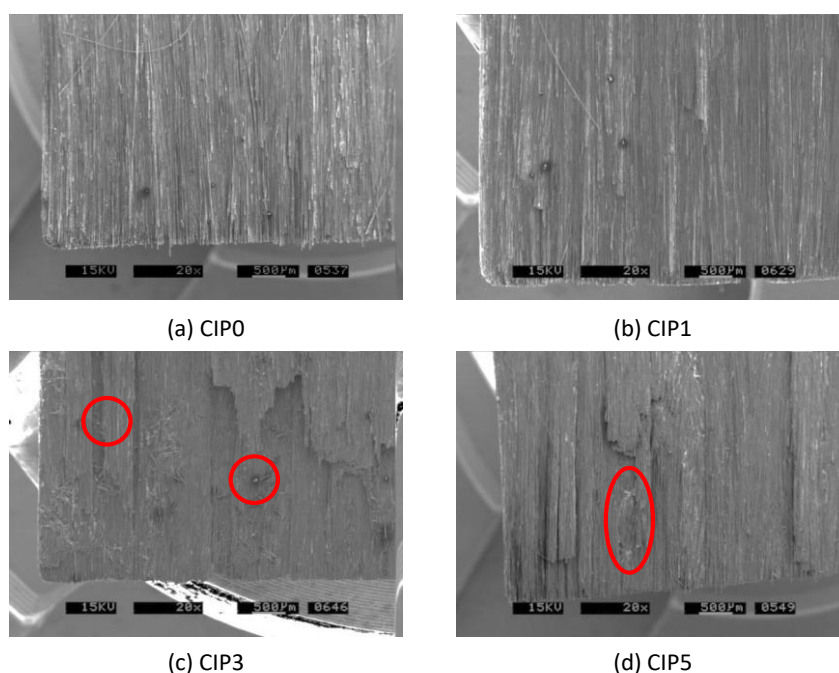

(a) CIP0

(b) CIP1

(c) CIP3

(d) CIP5

Figure 10. Fractured surfaces of SiC-C/C composites.

(a) CIP0   (b) CIP1
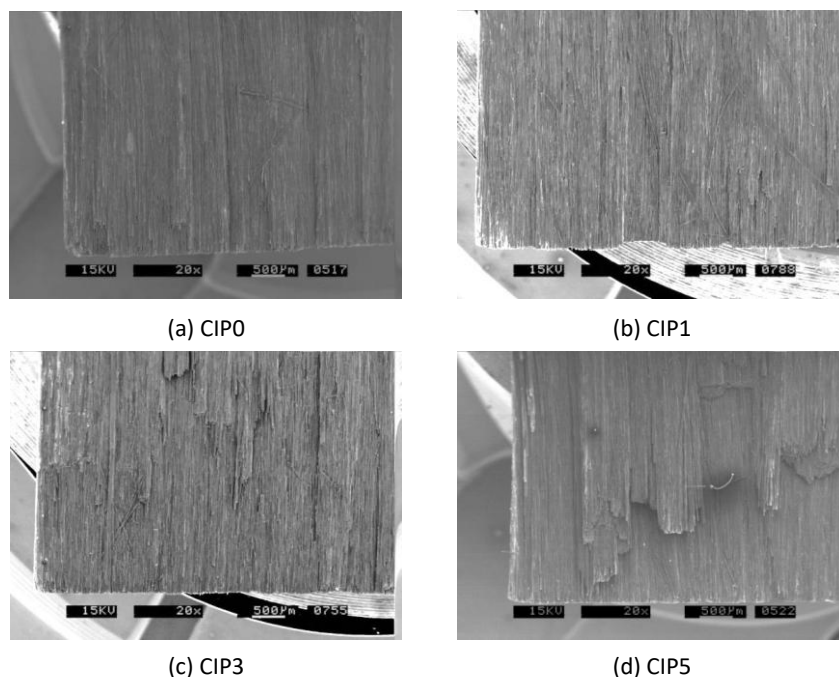
(c) CIP3   (d) CIP5

Figure 11. Fractured surfaces of C/C composites.

For both the composites, as the number of densification processes was increased, a dense matrix could be observed between the fibers and the fractured surface become rougher. A detailed observation of the fractured surfaces of the SiC-C/C composites confirmed that SiC nano-whiskers were present there. These results suggest that the inter-laminar shear strength of the SiC-C/C composites might have been improved due to the existence of these SiC nano-whiskers on the inter-laminar surfaces. In other words, the apparent shear strength of the composites was enhanced by promoting mechanical bridging between the laminar surfaces via the synthesized SiC nano-whiskers.

3.4. Microstructure of carbon matrix

Previous sections revealed that when the matrix of a SiC-C/C composite was modified with glass fibers, the improvement in bending characteristics and inter-laminar shear strength due to densification process was greater than that observed in the C/C composites. In this section, the question of why a greater improvement was observed in the SiC-C/C composites is addressed. As reported in Section 3.1, the decrease in pore volume and porosity of the SiC-C/C composites due to the densification process was also greater than that observed for the C/C composites. These results suggest that the microscopic structure of the composites may have been altered by the addition of glass fibers to their carbon precursor resins. To allow a more detailed examination of the microstructure of the composite matrix, a model specimen was used to investigate the microstructural changes that take place due to carbonization. Figure 12 shows a schematic illustration of the model specimen. This specimen consisted of C/C composites and a model matrix. The modified and unmodified precursor resins were placed between the C/C composites and cured. The model specimen was charred at 1773 K under the same conditions as those described in Section

2.2. After carbonization, the model specimen was divided at the position where the model matrix was obtained. The macrostructure of the model matrix was observed by SEM. Figure 13a,b show the observed macrostructures of the modified and unmodified carbon matrix, respectively. In the unmodified matrix, thermal cracking was observed mainly along the fiber direction. In the modified matrix, the vestiges of the added glass fiber and thermal cracking were both confirmed. Comparing the thermal cracks of both the specimens, the direction of thermal cracking in the SiC-C/C composite was more complex compared to that observed in the C/C composite. Moreover, due to the existence of vestiges of the added glass fiber, the coalescence of the thermal cracks was confirmed. When the densification process was performed, the thermal cracks would have provided flow paths for the impregnated resin. Therefore, the modified carbon matrix might have been more effectively densified by promoting good resin impregnation along the thermal cracks. Therefore, the densification by CIP treatment is effective for the SiC-C/C composites prepared by the proposed method. On the other hand, in C/C composites, when the densification process was performed, the thermal cracks in the matrix might be propagated due to pressure impregnation. Owing to the propagation of thermal cracks, the mechanical characteristics of the composites might have been initially degraded. However, as the densification process was repeated, the thermal cracks were finally bridged by the carbon matrix; therefore, the mechanical characteristics of the composites were improved.
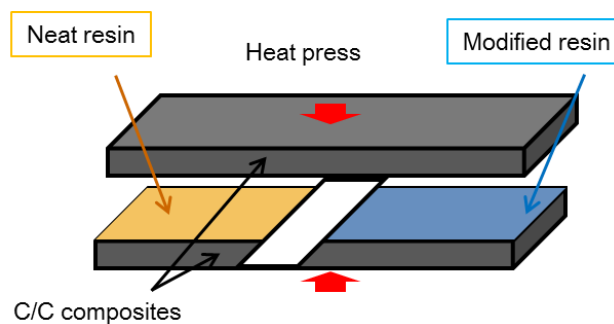
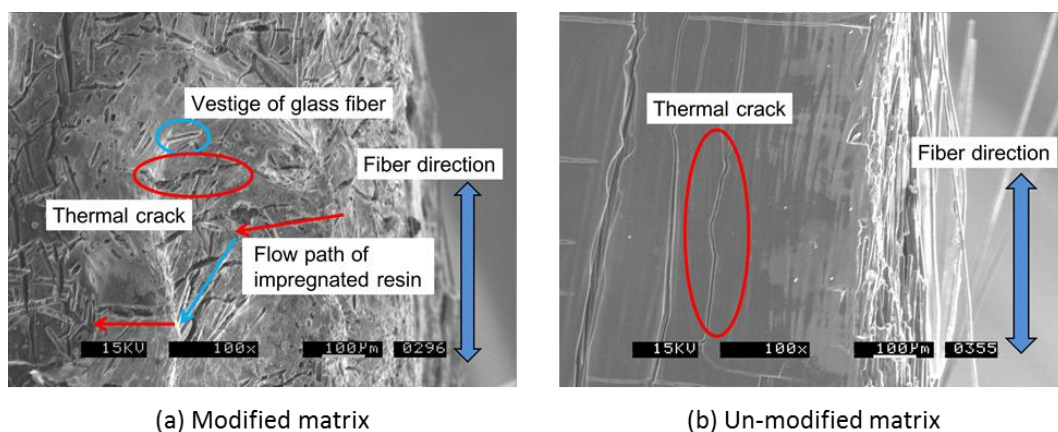

Figure 12. Schematic illustration of model specimen.

Figure 13. Microstructures of model matrix.

4. Conclusions

In this study, the densification availability and the effect of densification on the mechanical characteristics of SiC-C/C composites fabricated by the proposed method were investigated. The following conclusions have been drawn.

(1) By conducting the densification by CIP method, the porosity reduction of developed SiC-C/C composites was more obvious compared by that of C/C composites.

(2) Applying the densification process to the SiC-C/C composites prepared by the proposed method effectively improved their bending characteristics.

(3) The inter-laminar shear strength of the developed SiC-C/C composites might have been improved not only because of the densification process but also due to the existence of SiC nano-whiskers at the inter-laminar surfaces.

(4) The direction of thermal cracking in the developed SiC-C/C composites was complex compared to that observed in the C/C composites. By promoting good resin impregnation along these thermal cracks, the SiC-C/C composite might have been more effectively densified.

Acknowledgements

Conflict of interest

The authors declare that there is no conflict of interest regarding the publication of this manuscript.

References

1. Bussiba A, Kupiec M, Piat R, et al. (2008) Fracture characterization of C/C composites under various stress modes by monitoring both mechanical and acoustic responses. *Carbon* 4: 618–630.

2. Buchgraber W (2003) Carbon/Carbon composite friction discs for aerospace. *Materialwiss Werkst* 34: 317–321.

3. Don J, Wang Z (2009) Effect of anti-oxidant migration on friction and wear of C/C air craft brakes. *Appl Compos Mater* 16: 73–81.

4. Ishizawa S, Machida T (1997) Effect of Oxidation Degradation on Elevated-Temperature Strength of C/C Composite. *T Jpn Soc Mech Eng A* 63: 845–850 [in Japanese].

5. Bacos MP (1993) Carbon-carbon composites oxidation behavior and coatings protection. *J Phys IV France* 03: C7-1895-C7-1903.

6. Kim SY, Han IS, Woo SK, et al. (2013) Wear-mechanical properties of filler-added liquid silicon infiltration C/C-SiC composites. *Mater Design* 44: 107–113.

7. Zhao K, Li K, Wang Y (2013) Rapid densification of C-SiC composite by incorporating SiC nanowires. *Compos Part B-Eng* 45: 1583–1586.

8. Vignoles GL, Goyhénèche JM, Sébastian P, et al. (2006) The film-boiling densification process for C/C composite fabrication: From local scale to overall optimization. *Chem Eng Sci* 61: 5636–5653.
9. Stadler Z, Krnel K, Kosmac T (2007) Friction behavior of sintered metallic brake pads on a C/C-SiC composite brake disc. *J Eur Ceram Soc* 27: 1411–1417.
10. Zhang J, Xu Y, Zhang L, et al. (2007) Effect of braking speed on friction and wear behaviors of C/C-SiC composites. *Int J Appl Ceram Tec* 4: 463–469.
11. Zhou X, Zhu D, Xie Q, et al. (2012) Friction and wear properties of C/C-SiC braking composites. *Ceram Int* 38: 2467–2473.
12. Kawai C, Igarashi T (1991) Oxidation resistant coating of TiC-SiC system on C/C composite by chemical vapor deposition. *J Ceram Soc Jpn* 99: 390–394 [in Japanese].
13. Utunomiya Y, Obunai K, Fukuta T, et al. (2016) Mechanical Characteristics of C/C Composites Modified with Micro-Sized Glass Fibers. *Adv Exp Mech* 1: 126–130.
14. Obunai K, Mikami D, Fukuta T, et al. (2016) Mechanism of SiC synthesisation at C/C composites modified with glass fiber during char condition. JSMS Composites Young Research Symposium [in Japanese].
15. Kimura M, Obunai K, Okubo K, et al. (2014) Moderation of Dependence of Frictional Coefficient of C/C Composite on Temperature due to Addition of Glass Fibers into Carbon Precursor of Phenolic Resin. Proceedings of ACCM9, ACCM9-C-007.
16. Li M, Matsuyama R, Sakai M (1999) Interlaminar shear strength of C/C composites: the dependence on test methods. *Carbon* 37: 1749–1757.
17. Thielicke B, Soltesz U, Krenkel W, et al. (1999) Creep of a C/C-SiC composite under interlaminar shear loading at high temperatures. Proceedings of ICCM12.
18. Nakamura C, Sakai Y, Kishi T (2012) Study on the effects of chemical and physical property of concrete on the behavior of water. *Cement Sci Concrete Technol* 66: 444–451 [in Japanese].